A least-squares spectral collocation scheme with improved stability for the Stokes and the Navier-Stokes equations

Thorsten Kattelans* and Wilhelm Heinrichs†

*University of Duisburg-Essen, Engineering Mathematics, Universitaetsstrasse 3, D-45117 Essen, Germany.
E-mail: thorsten.kattelans@uni-due.de
†University of Duisburg-Essen, Engineering Mathematics, Universitaetsstrasse 3, D-45117 Essen, Germany.
E-mail: wilhelm.heinrichs@uni-due.de

Abstract. We consider a new least-squares spectral collocation scheme for the Stokes and the Navier-Stokes equations. By introducing the Clenshaw-Curtis quadrature rule for imposing the average pressure to be zero we reduce the condition numbers of the over-determined systems. All computations are performed with an explicit scheme and saves a lot of CPU time compared to implicit schemes. We compare two different types of interface conditions and two different types of decompositions of the domain. The over-determined linear systems of equations are solved by *QR* decomposition. Since we avoid the normal equations (squared conditions numbers) we improved the quality of approximation. Finally, our scheme is successfully applied to the regularized and lid-driven cavity flow.

Keywords: Navier-Stokes equations, least-squares, spectral collocation, explicit scheme, interface conditions, decomposition of the domain, direct solver, improved stability, Clenshaw-Curtis quadrature
PACS: 47.11.Kb

THE STOKES AND NAVIER-STOKES EQUATIONS

In order to apply least-squares we consider the Stokes and Navier-Stokes equations in a first-order formulation. For the bounded domain $\Omega \subset \mathbb{R}^2$ the Navier-Stokes equations are given by

$$\frac{\partial \mathbf{u}}{\partial t} + \mathbf{u}\cdot\nabla\mathbf{u} + \nu\nabla\times\omega + \nabla p = \mathbf{f} \quad \text{in } \Omega\,,\ t\in[0,t_{end}] \tag{1}$$

$$\nabla\cdot\mathbf{u} = 0 \quad \text{in } \Omega\,,\ t\in[0,t_{end}] \tag{2}$$

$$\omega - \nabla\times\mathbf{u} = 0 \quad \text{in } \Omega\,,\ t\in[0,t_{end}] \tag{3}$$

where $\mathbf{u}^T = [u_1, u_2]$ denotes the velocity vector, p the pressure, ω the vorticity, $\mathbf{f}^T = [f_1, f_2]$ the forcing term and $\nu = \frac{1}{Re}$ the kinematic viscosity. Here it is assumed that the density equals unity. For the Stokes equations the only difference is that they do not contain the convective term in (1). Since the pressure is through (1)-(3) only determined up to a constant for the Stokes respectively Navier-Stokes equations we have to introduce an additional condition for the pressure. One procedure is to impose the pressure at an arbitrary point of the considered domain. Another way of dealing with the pressure constant is imposing the average pressure to be zero; i.e.,

$$\int_\Omega p\,d\mathbf{x} = 0. \tag{4}$$

LEAST-SQUARES SPECTRAL COLLOCATION

Spectral methods employ global polynomials for the numerical solution of differential equations. Hence they give very accurate solutions for smooth solutions with relatively few degrees of freedom. For analytical data exponential convergence can be achieved. For the spectral approximation we introduce the polynomial subspace
$\mathbb{P}_N = \{\text{Polynomials of degree} \le N \text{ in both variables } x_1, x_2\}$. Now all unknown functions are approximated by polynomials of the same degree N, i.e., u_1, u_2, ω, p are approximated by interpolating polynomials u_1^N, u_2^N, ω^N, $p^N \in \mathbb{P}_N$. Furthermore, we have to introduce the standard Chebyshev Gauss-Lobatto collocation nodes which are explicitly given by $(\xi_i, \eta_j) = \left(-\cos\left(\frac{i\pi}{N}\right), -\cos\left(\frac{j\pi}{N}\right)\right)$, $i, j = 0, \ldots, N$. In the following we write the spectral derivatives. First

we have to introduce the transformation matrices from physical space to coefficient space. Since we employ a Chebyshev expansion we obtain the following matrix: $T = (t_{i,j}) = \left(\cos\left(j\frac{(N-i)\pi}{N}\right)\right), \quad i,j = 0,\ldots,N$. Further, we need the differentiation matrix in the Chebyshev coefficient space which is explicitly given by $\hat{D} = (\hat{d}_{i,j}) \in \mathbb{R}^{N+1,N+1}$ with

$$\hat{d}_{i,j} = \begin{cases} \frac{2j}{c_i} & , \quad j = i+1, i+3, \ldots, N \\ 0 & , \quad \text{else} \end{cases} \quad \text{and} \quad c_i = \begin{cases} 2 & , \quad i = 0 \\ 1 & , \quad \text{else} \end{cases} .$$

Now we are able to write explicitly the spectral derivative matrix D for the first derivative which is given by $D = T\hat{D}T^{-1} \in \mathbb{R}^{N+1,N+1}$. The spectral transformation operator T can be efficiently evaluated by Fast Fourier Transformations (FFTs) in $\mathcal{O}(N \log N)$ arithmetic operations. We further introduce the identity matrix $I \in \mathbb{R}^{N+1,N+1}$. By tensor product representation $A \otimes B = (Ab_{i,j})_{i,j}$ we are now able to write the spectral derivatives:

$$\frac{\partial}{\partial x} \cong D_1 := D \otimes I \quad , \quad \frac{\partial}{\partial y} \cong D_2 := I \otimes D. \tag{5}$$

Furthermore, we have to discretize (4). This is performed by the well-known Clenshaw-Curtis quadrature rule, see [9], [10]. We use the Clenshaw-Curtis quadrature rule since this is the appropriate quadrature rule for the Chebyshev Gauss-Lobatto nodes. The advantage of the Chebyshev nodes is the fact that they are explicitly given and FFTs are available. One could also use Gaussian quadrature, in the numerical experiments there is no big difference. Since we want to simulate the lid-driven cavity flow (non-smooth solution with corner singularities) we have to decompose the domain Ω into sub-elements. We performed our simulations with two different domain decompositions and a different number of elements K^2. Figure 1 shows the different decompositions for equidistant elements and Chebyshev Gauss-Lobatto (CGL) elements. Because we decompose the domain Ω into K^2 sub-elements we have to transform the collocation

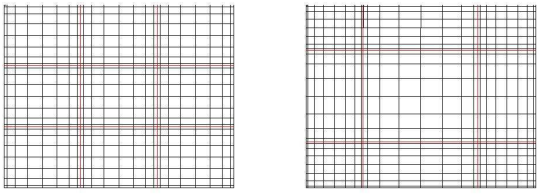

FIGURE 1. Different types of decomposition of the domain Ω into $K^2 = 9$ elements with $N = 8$. Left: equidistant elements, right: CGL elements

nodes (ξ_i, η_j) and the spectral derivative matrices D_1, D_2 to the corresponding elements by a linear mapping. Now it is an easy task to write the discrete version of the PDE with the here considered decompositions of the domain, see [10]. For time integration we use BDF schemes and for the non-linear convective term $\mathbf{C} = (\mathbf{u} \cdot \nabla)\mathbf{u}$ of the Navier-Stokes equations we used an explicit scheme (BDF scheme for viscous term combined with extrapolation based on an Adams-Bashforth technique for convective term), see [9]. At the interfaces between the elements, we require two different types of interface conditions and compare the numerical results. The two different interface conditions are:

1. C^1 interface conditions, i.e. we require continuity of both the functions and normal derivatives of u_1, u_2, continuity of p and no explicit interface conditions for ω.
2. C^0 interface conditions, i.e. we require continuity of u_1, u_2, continuity of p and continuity of ω.

Since we particularly enforce the collocation conditions on the interfaces and on the boundary $\partial\Omega$ and we additionally enforce the pointwise continuity on the interfaces and enforce the values of the velocity on the boundary we get really over-determined linear systems of equations, see [9]. The advantage of least-squares techniques is amongst others that they do not require a stabilization, see e.g. [1].

NUMERICAL SIMULATIONS

Since it is well-known that the spectral derivative matrices have large condition numbers we have to care about reducing them. We found out that the additional integral pressure condition (4) leads to linear systems of equations with

reduced condition numbers compared to imposing the pressure in one discrete point (see figure 2, left). Furthermore, we use the *QR* decomposition for solving the over-determined linear system of equations to avoid solving with the corresponding normal equations (see [7],[8]) with squared condition numbers (see figure 2, middle and right). Because of avoiding the large condition numbers we achieved better approximations since our scheme is not as sensitive as the scheme where the pressure is set in one discrete point of Ω and the linear systems of equations are solved with normal equations. A further disadvantage of setting the pressure in one discrete point of the cavity is, we do not know the pressure if we consider the cavity flow problems. All computations for Stokes equations are performed on equidistant elements since we only consider smooth examples. The computations for Navier-Stokes equations are done on the two different element types. For smooth examples there is no nameable difference between C^1 and C^0 interface conditions.

The Stokes equations

With this new scheme we first numerically solve the **steady Stokes equations** for the smooth example given in [9]. The computations has shown the exponential convergence of our scheme. Concerning computational costs we compare solving the linear systems of equations with *QR* decomposition, pseudoinverse and normal equations. The results are that using *QR* decomposition and using pseudoinverse lead to the same accuracy but using pseudoinverse requires much more computing time, see [9]. Using normal equations requires less time but does not show such good accuracies (see figure 2, middle and right). From a theoretical point of view it is clear that all of the three solving techniques must lead to the same results. Because of the influence of round-off errors we do not obtain the same approximations with the three solvers. Furthermore, we compare both schemes to show numerically the better performance of the one with Clenshaw-Curtis quadrature and *QR* decomposition.

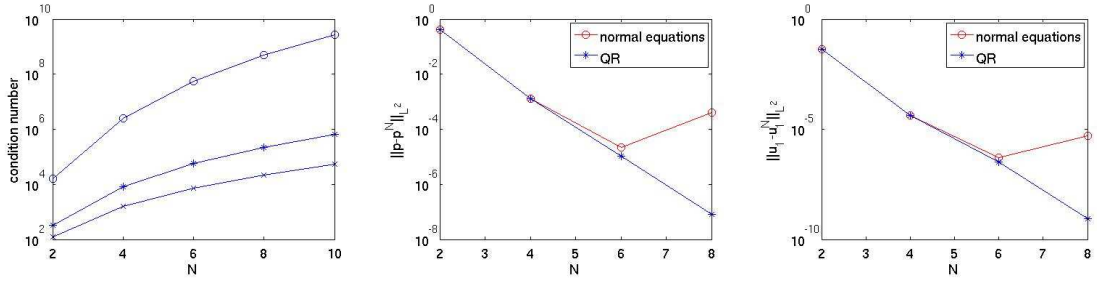

FIGURE 2. *The Stokes equations ($Re = 1$). Left ($K^2 = 4$): Condition numbers with Clenshaw-Curtis quadrature for the pressure $(\times)$, with imposing the pressure in one point $(*)$ and normal equations (o); middle ($K^2 = 36$): L^2-error of the pressure (with Clenshaw-Curtis quadrature) on equidistant elements; right ($K^2 = 36$): L^2-error of the velocity component u_1 (with Clenshaw-Curtis quadrature) on equidistant elements*

Next, we consider the **unsteady Stokes equations** where we use a second-order BDF scheme for time integration. Here, our scheme shows a very good accuracy if a Δt-scaling of the momentum equations is introduced, see [9]. Without scaling our scheme becomes divergent since the incompressibility condition (2) is lost during time integration.

The Navier-Stokes equations

For the Navier-Stokes equations we first consider the steady and smooth example given in [9]. Our computations has shown the high spectral accuracy of our new (i.e., with Clenshaw-Curtis pressure condition and with *QR* decomposition) scheme on equidistant and CGL elements. All computations of the Navier-Stokes equations are performed with the explicit scheme described above and with regularization of the linear system of equations by the Clenshaw-Curtis quadrature rule for the pressure. Our next test case is the **"regularized cavity flow"** for Reynolds numbers $Re = 100$ and $Re = 400$ where the fluid velocity on the edge $y = 1$ of cavity $\Omega := (0,1)^2$ is given by $u_1(x,1) := -16x^2(1-x)^2$ and $u_2(x,1) := 0$. On the other three edges the velocity equals zero. We compare our results with the benchmarks in the literature and obtained the very good performance of our scheme. We found that our scheme works best on CGL elements (especially for higher Reynolds numbers) since these elements resolve the singularities in the corners $(0,0)$, $(0,1)$, $(1,1)$ and $(0,1)$ in the best way. In table 1 we compare our results (64 equidistant and CGL elements with C^1 respectively C^0 interface conditions) with the benchmarks of Botella in [2]. When the steady state is reached (see [9]),

the stream function Ψ is computed by the solution of a Poisson equation where the right-hand side equals $-\omega$ and zero boundary conditions are given. For the numerical solution of this second-order system we first transform it into an equivalent first-order system and then again use our least-squares scheme for solving this system. The interface conditions for this Poisson equation are the same as for the Navier-Stokes equations. For a more in-depth description see [9]. The last challenging test case for our new scheme is the **"lid-driven cavity flow"** for Reynolds numbers $Re = 100$ and $Re = 1000$ where the fluid velocity on the edge $y = 1$ of the cavity $\Omega := (0,1)^2$ is given by $u_1(x,1) := -1$ and $u_2(x,1) := 0$. On the other three edges the velocity equals zero. Because of this boundary conditions we have two sharp singularities in the two upper corners and two weaker singularities in the two lower corners of the cavity (previous work for spectral element methods has been done in [4]-[6], [11]-[12]). The comparison of our approximations with the benchmarks show the good performance of our scheme for Reynolds numbers up to $Re = 1000$. As our simulations has shown the CGL elements are preferable since they resolve the singularities in the best way if the functions have sharp gradients in the vicinity of the boundary. In table 2 we show the extrema of the velocity for the lid-driven cavity flow through the centerlines $x = 0.5$ and $y = 0.5$ of the cavity for $Re = 1000$ on 64 equidistant and CGL elements with C^1 and C^0 interface conditions. In [3] a subtraction method was used and so we do not obtain such good values since we have placed all variables in the singularities. Comparing table 1 and table 2 we see that C^1 interface conditions are preferable, if the functions have strong variations (lid-driven cavity flow) in some regions. The reason is that the stronger (C^1) interface conditions transport the information of the functions in a smoother way to the other elements.

TABLE 1. Maximal value of the stream function Ψ in Ω and maximal value of the vorticity ω on the edge $y = 1$ for the regularized cavity flow with Re=400 on 64 equidistant and CGL elements with C^1 respectively C^0 interface conditions

$\max_{(x,y)\in\Omega} \lvert\Psi(x,y)\rvert$	$\max_{x\in[0,1]} \omega(x,1)$	**Elements**	**Interface conditions**
$8.63\times10^{-2}\,(0.44,0.62)$	$25.61\,(0.62)$	Equidistant	C^1
$8.55\times10^{-2}\,(0.40,0.60)$	$24.81\,(0.64)$	CGL	C^1
$8.56\times10^{-2}\,(0.40,0.60)$	$24.81\,(0.64)$	CGL	C^0
$8.55\times10^{-2}\,(0.40,0.60)$	$24.78\,(0.65)$	[2]	

TABLE 2. Extrema of the velocity for the lid-driven cavity flow (Re=1000) through the centerlines $x = 0.5$ and $y = 0.5$ of the cavity on 64 equidistant and CGL elements with C^1 respectively C^0 interface conditions

$u_{1,max}, y_{max}$	$u_{2,max}, x_{max}$	$u_{2,min}, y_{min}$	**Elements**	**Interface conditions**
0.500,0.188	0.497,0.867	-0.640,0.094	Equidistant	C^1
0.397,0.157	0.391,0.843	-0.538,0.092	CGL	C^1
0.407,0.157	0.404,0.854	-0.550,0.092	CGL	C^0
0.389,0.172	0.377,0.842	-0.527,0.091	[3]	

REFERENCES

1. P. B. Bochev, and M. D. Gunzburger, *SIAM Rev.*, **40**, 789–837 (1998).
2. O. Botella, *Comput. Fluids*, **26**, 107–116 (1997).
3. O. Botella, and R. Peyret, *Comput. Fluids*, **27**, 421–433 (1998).
4. M. M. J. Proot, and M. I. Gerritsma, *J. Comput. Phys.*, **181**, 454–477 (2002).
5. M. M. J. Proot, and M. I. Gerritsma, *J. Sci. Comput.*, **17**, 285–296 (2002).
6. M. M. J. Proot, and M. I. Gerritsma, *Numer. Algorithms*, **38**, 155–172 (2005).
7. W. Heinrichs, *J. Sci. Comput.*, **21**, 81–90 (2004).
8. W. Heinrichs, *J. Eng. Math.*, **56**, 337–350 (2006).
9. W. Heinrichs, and T. Kattelans, *J. Comput. Phys.*, **227**, 4776–4796 (2008).
10. T. Kattelans, *Spektrale Least-Squares Verfahren fuer inkompressible Navier-Stokes-Gleichungen*, diploma thesis, University of Duisburg-Essen, Essen, Germany (2007).
11. J. P. Pontaza, and J. N. Reddy, *J. Comput. Phys.*, **190**, 523–549 (2003).
12. J. P. Pontaza, and J. N. Reddy, *J. Comput. Phys.*, **197**, 418–459 (2005).